

DESIGN OF ANTENNA ARRAY FOR BREAST TUMOR DETECTION

Ganadiko M. Bayero¹, Hon Kah Wye¹ & Sanjay Sree¹
¹*Infrastructure University Kuala Lumpur, Malaysia*

ABSTRACT

Breast cancer has in recent time become a leading cause of mortality among women, which necessitate a suitable means of early detection for fast and effective treatment. X-ray Mammography, which is currently the commonly used method of breast screening, comes with limitations such as missed detection because of poor malignant/benign cancer tissue contrast as well as exposure of the breast to radiation. Microwave imaging serves as a better alternative to X-ray mammography, because of its harmlessness to humans and better detection. In this paper, a study on the effects of the bending of the microstrip antenna array for breast tumour detection is presented. The antenna array was designed with resonant frequencies of 2.4 GHz and return loss less than -35 dB. The antenna is simulated by introducing a truncated edge slot at the network feedline of the conformal antenna array. The result shows that the proposed antenna design is capable of detecting the breast tumour with improved characteristics compared to other designs available in the literature. The simulation analysis of the designed antenna is carried out using CST software. The capabilities and bending effect of this antenna for detecting different tumour sizes is investigated and its potential is highlighted. The results obtained with this antenna design makes it suitable antenna for breast tumour detection

Keywords:

Breast Tumour Detection, Microstrip Patch Antenna, Antenna Array, CST, UWB Antenna, Biomedical application.

INTRODUCTION

Early diagnosis of breast tumour in women is very important for proper and effective treatment. This, however, necessitates locating the precise position and size of the tumour in the breast since tumour is tiny at early stage; the knowledge of its precise location is chiefly required (Srinivasan and Gopalakrishnan, 2019). Microwave imaging (MWI) is an encouraging technique because it is able to detect the precise location of the tumour, and also, distinguish between normal and cancerous tissues from their dielectric properties (K. Ouerghi, A. Smida, R. Ghayoula and N. Boulejfen 2017). Unlike the other conventional methods of diagnosis of tumour such as X-ray, MRI, the Microwave Imaging (MWI) method is non-ionizing, non-invasive and reasonably cheaper cost. Therefore, this purpose serves as a driving force and urge to explore more research areas in microwave imaging (MWI) for early detection of breast tumour. There are two approaches in Microwave Imaging (MWI): Linear (Pierri, Leone and Persico, 2000) and nonlinear (Khalil and Jiadong, 2014) imaging methods, these two approaches have both been applied to reconstruct the electrical properties of the breast from measured data.

The microwave imaging techniques measures the scattered field from the tumour illuminated by electromagnetic waves radiated from transmitting antennas. The scattered signals strongly depends on many factors, including the environment, dielectric properties of the object, signal strength (Zhong Qing Zhang et al., 2003). For a given signal source in a certain environment, the scattered signal depends on the electrical properties of the object. (Shrestha et al., 2012). There are information contained in the scattered field as regard the conductivity and dielectric properties of the breast that can be reconstructed using imaging algorithms. The breast tumour have very distinct electrical properties, such as permittivity and conductivity, they are possible to be detected by analysing the

scattered signals. It is left for Medical practitioners to examine the electrical properties reconstructed from the scattered field for tumour detection.

In this paper, we develop an array antenna consisting of four (4) element antennas to form a 1X4 array antenna, two (2) element antennas to form 1X2 array antennas and a single element patch antenna. The array antenna is perfectly suited for microwave imaging (MWI) technology due to its numerous advantages such as extremely low profile, fairly inexpensive, and easy to fabricate/manufacture. Due to their sizes, the array antenna was fabricated on a printed circuit board (PCB) using photo-etching technology. The array antenna was designed to operate at a single frequency. The geometry of these array antenna is chosen for the best illumination to the target in near field measurements. Rogers RO 4003C material is used for substrate with dielectric constant 3.38. The choice of Rogers RO 4003C is because a flexible substrate is required so as to meet the objective of having a bendable antenna around the breast. The aim is to investigate the effect of bending the array antenna around the breast. The array antenna is designed using CST Microwave studio for simulations. The array antenna were chosen and used for our microwave imaging system, because the use of microstrip arrays in biomedical applications help enhance the performance of the antenna by increasing the gain, enhancing the directivity scanning of the beam and other function that are limited in a single element (K. Ouerghi et al, 2017). Additionally, the array antenna has good impedance matching, efficiency and proper bandwidth.

SYSTEM CONFIGURATION AND RESULTS

Computer simulation technology (CST MWS) software is used to design antennas and systems models, as well as investigates the effect of the bending on the antenna. A preliminarily designed single element patch antenna is shown in figure 1. Depicted in table 1 is the compressive details of antenna array specifications.

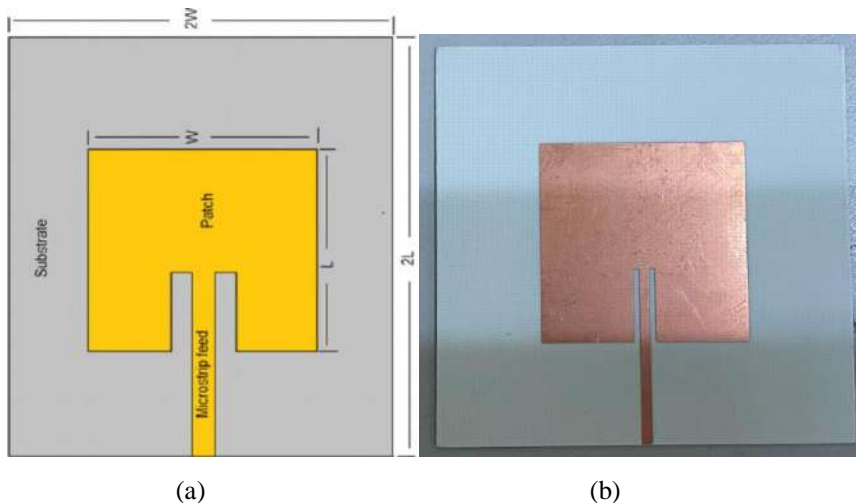


Figure 1. (a) Geometry of the single patch antenna: $W = 34.50$, $L = 31.53$, Substrate = Rogers RO 4003C, Patch and feed = Copper, Inset Length = 12.20, Gap = 1.57; (b) Front view of the fabricated patch antenna.

The operation frequency of the designed patch array antenna is 2.4 GHz. To enhance the accuracy of the detection, the single element of the microstrip antenna was optimized to an array antenna. And this has resulted the need to balance the gain as well as the size of the array antenna.

The SMA connector was soldered to the bottom of the feedline. Take into consideration that after the results of the single element has shown to be satisfactory, the single element was optimized to design a 1x2 array antenna, which was subsequently optimized to design the 1x4 array antenna as shown in figure 2(a) and figure 2(b) respectively.

Table 1: Design specifications of the antenna array design.

| Design Specification | Value (mm) |
|-----------------------------|------------|
| Patch antenna length | 31.53 |
| Patch antenna width | 34.50 |
| Ground plane length | 38.75 |
| Ground plane width | 42.00 |
| Inset length | 12.20 |
| Roger board thickness | 0.508 |
| Copper thickness of patch | 0.035 |
| Gap between inset and patch | 3.8 |
| 50 Ω feedline length | 23.3 |
| 50 Ω feedline width | 2.6 |

Figure 2(a) shows the antenna array design in CST while figure 2(b) shows the fabricated antenna array with SMA connector. Measured and simulated S-parameters of the 1x4 antenna array are shown in Figure 3. It can be observed that there is a sound agreement between the simulated and measured S-parameters of the 1x4 antenna array. Interestingly, as it can be seen, both the simulated and measured antenna array resonates at 2.4 GHz.

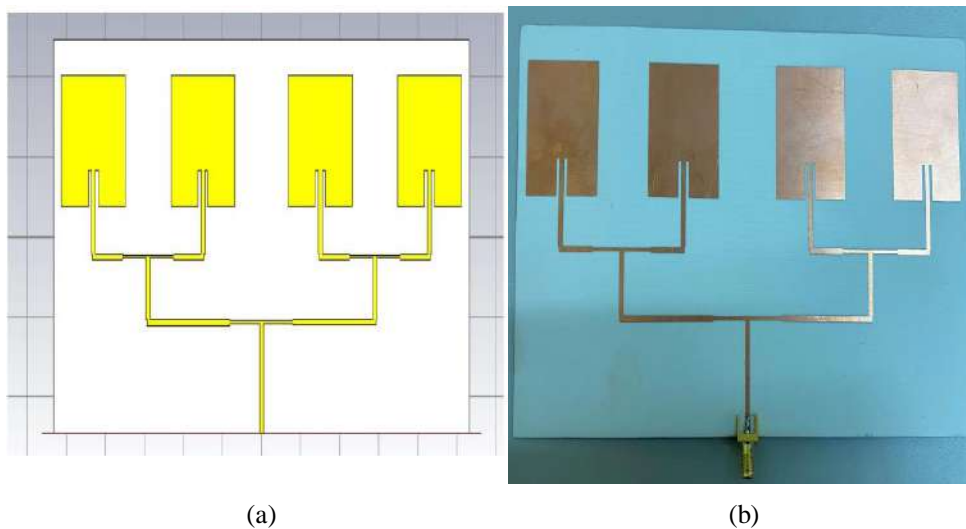


Figure 2. (a) Simulated 1x4 antenna array (b) Fabricated 1x4 antenna array with SMA connector.

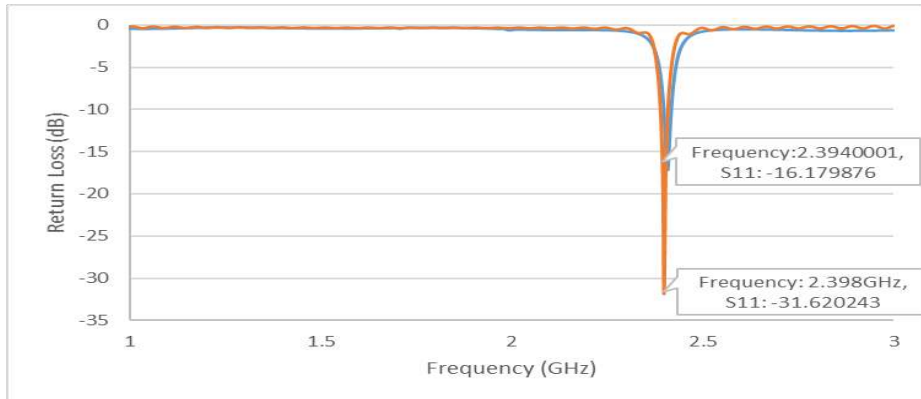


Figure 3: Measured and simulated S-parameters of the 1x4 antenna array

In order to check the performance of the array antenna as regards to the bending effect on the detection of breast tumour, a dielectric cylinder is deployed at the back of the antenna array. Note that the curvature of the array varied in terms of degrees. The height and radius of the cylinder depends on the degree of the curvature. The curvature of the antenna array simulated in CST and also the measured are shown in figure 4. Additionally, table 2 and table 3 depicts the simulated and experimental real measured value of different curvatures with resonating frequency and return loss as well. Notice, that from both the tables we can observe that there is a change in resonance frequency when the radius of the curvature increases. Figure 4(a) shows the curvature of antenna array design in CST while figure 4(b) shows the curvature of fabricated antenna array. Also shown in figure 5 is the comparison of the bending effect of the fabricated array antenna in S-parameters.

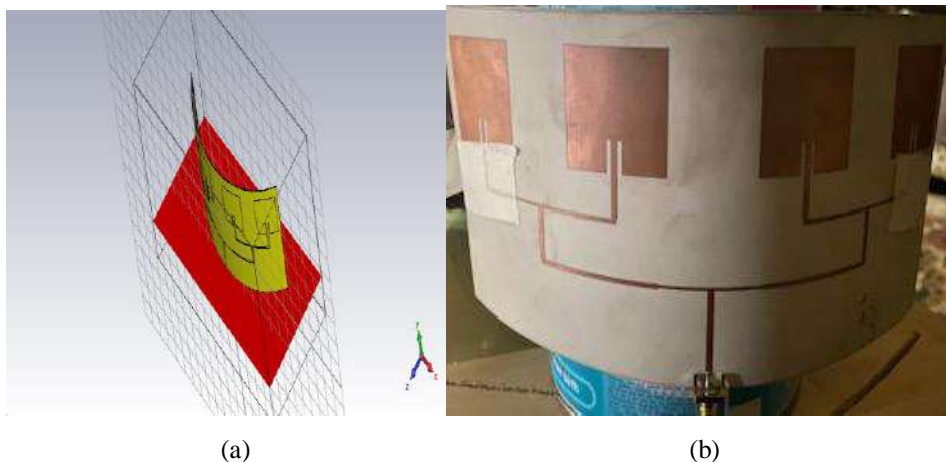


Figure 4. (a) Simulated 1x4 antenna array (b) Fabricated 1x4 antenna array with SMA connector.

Table 2: The simulated value of curvature of 1 x 4 array.

| Bending Degree | Curvature Radian | Radius(r) $S = r\theta$ | Resonance Frequency (GHz) | Return Loss S11 |
|----------------|------------------|----------------------------|---------------------------|-----------------|
| 0 | - | - | 2.408 | -37.37 |
| 5 | 3.055 | 89.95 | 2.404 | -24.21 |
| 7 | 3.0019 | 90.85 | 2.382 | -28.92 |
| 10 | 2.967 | 92.65 | 2.398 | -31.62 |
| 13 | 2.837 | 94.33 | 2.396 | -24.69 |
| 15 | 2.880 | 95.45 | 2.304 | -22.81 |

Table 3: The measured value of curvature of 1 x 4 array.

| Bending Degree | Radius (r) $S = r\theta$ | Resonance Frequency (GHz) | Return Loss S11 |
|----------------|-----------------------------|---------------------------|-----------------|
| 0 | - | 2.426 | -35.78 |
| 5 | 89.95 | 2.400 | -13.19 |
| 7 | 90.85 | 2.441 | -14.56 |
| 10 | 92.65 | 2.394 | -16.17 |
| 13 | 94.33 | 2.484 | -16.01 |
| 15 | 95.45 | 2.399 | -15.72 |

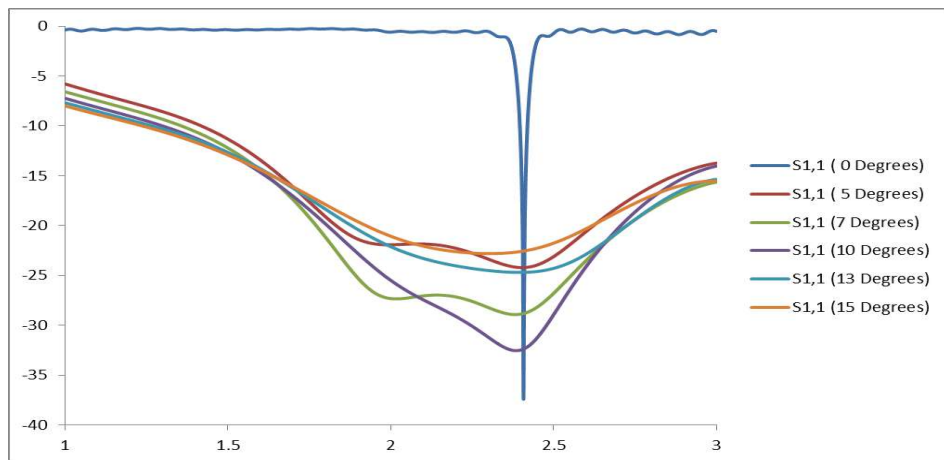


Figure 5: Measured S11 results of curved antenna array

BREAST PHANTOM DESIGN

A model of the breast was created using the CST microwave studio software as shown in Figure 6. The model of the breast is an approximate replication of a human breast. Varieties of breast phantoms are distinguished by the critical electrical properties that are the relative permittivity ϵ_r and the conductivity ' σ '. As clearly seen in figure 6, the geometry of the microstrip antenna, the homogeneous 3D model of the breast phantom (Figure 6a) and the breast phantom design in CST (Figure 6b) consisting of skin, tissue and tumour were determined using the different dielectric properties. Tabulate the dielectric properties of the concept was developed as a half-sphere with 3 mm thick skin layer and 25 mm outer radius. Within the skin layer is found a fibro-glandular breast fatty tissue layer of radius 22 mm. A plane wave proceed towards the model through the z-axis, and the field is located at 4 mm. The breast model is stimulated by the stimulus of the plane wave. The plane wave is transmitted across the device and provided by the ground afterwards. A tumour is positioned as a 10 mm diameter ring inside the fibro-glandular breast fatty tissue membrane. Table 4 illustrate the information of breast phantom dielectric properties.

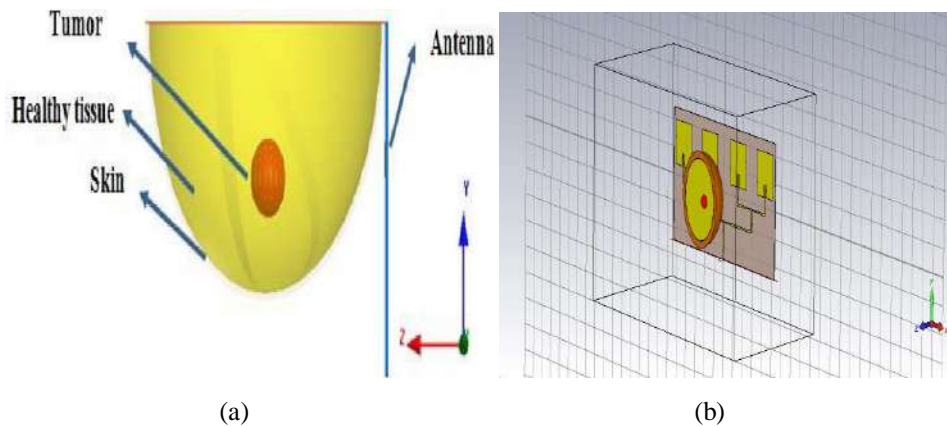


Figure 6: (a) Breast model with tumour; (b) Breast phantom design in CST

Table 4: Breast phantom dielectric properties

| Parameters | ϵ_r | σ (S/m) |
|------------|--------------|----------------|
| Skin | 36.58 | 2.3404 |
| Tumour | 67 | 49 |
| Fatty skin | 4.8393 | 0.26229 |

BREAST PHANTON DESIGN FOR TUMUOR IDENTIFICATION

In the construction of a breast phantom, three different layers were considered, these are; skin, fat, and tumour. But the silicon bra act as the skin in the designed phantom. The fat and tumour of the breast were fabricated and measured based on the procedures presented by (Islam, M. S, 2018). The dielectric properties of numerous tissues are considered by permittivity, which is the mean of complex-valued dielectric, as stated in Eqn (1)

$$\epsilon(\epsilon = \epsilon_r + i\sigma/\omega\epsilon_0) \quad (1)$$

Where ϵ_r represents the dielectric constant and σ denotes the conductivity of the tissue against frequency. The dielectric permittivity of vacuum here is ϵ_0 , and the angular frequency is ω . The image of the fabricated homogenous phantom is illustrated in figure 7.

For the fat and tumour, Sodium chloride (NaCl), polyethylene powder, agar powder, xanthan gum, sodium dehydroacetate monohydrate, and distilled water are used. Polyethylene powder is used to adjust the permittivity and NaCl to improve the conductivity. Agar is used to keep the shape of the phantom by preventing separation of water content, xanthan gum is used as a thickener and sodium dehydroacetate monohydrate as a preservative. The materials which alter the dielectric properties of this method are NaCl, polyethylene powder, agar, and distilled water, and they are the main ingredients in the fabrication of the fat and tumour. These materials are also natural to fabricate and possess high mechanical properties. The selected materials make it easy to produce the fat and tumour inside the breast phantom although different concentrations of the materials are used for both layers.



Figure 7: Developed homogenous breast phantom with tumour

EXPERIMENTAL SETUP AND RESULTS

An automated microwave imaging system was used for experimental validation. The breast phantom is placed under the antenna array after the antenna has been perfectly set up with the vector network analyser as shown in figure 8(a). Figure 8(b), presents the proposed experimental set-up on how the antenna array is bent around the breast phantom. Recall that, one of the objectives of this thesis is to investigate the effectiveness of the antenna array in a curved position around the breast phantom. The parameters of VNA are set as the IF-bandwidth is 10 Hz, the output power is 10 dBm, and the frequency range is 2 to 3 GHz. The microwave pulse is transmitted to the phantom from the transmitting antenna, simultaneously the reflected backscattered signals are collected by the same receiving antennas. The transmission parameters depend entirely on the antenna path. Most of the reflected parameters present the shallow depths under the skin layer. The signals are bounced off to the opposite side of breast phantom and attenuated significantly. The reflected signals can perfectly be detected by the antenna which has higher gain, directional radiation pattern, and lower reflection coefficient. Shown in figure 9 is location of the tumour inside the breast tissue structure (2D Image) (9a) Top view of breast model (9b) 2D Image for each breast tissue for different value of reflected power S11 value. In this research, the antenna array was tested in five different bending degrees, the five different bending degrees are perfectly chiselled into a fine wood, so as to enable easy bending

as shown in Figure 8(b). Subsequently, the comparison of S11 of the antenna array in all the bent degrees on the breast phantom is presented in Figure 10 while Table 5 outlines the overall antenna performance.

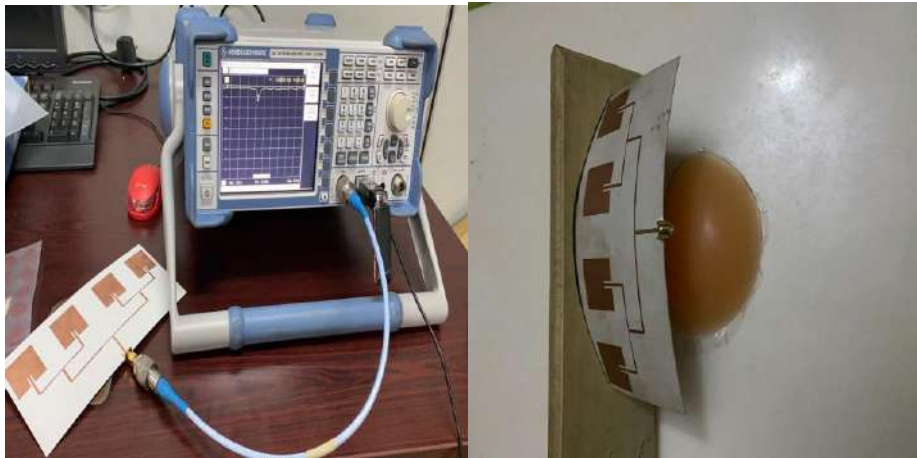


Figure 8: The Experimental setup. (a) Breast phantom under the antenna array after the antenna has been set up with vector network analyser. (b) presents how the antenna array is bent around the breast phantom

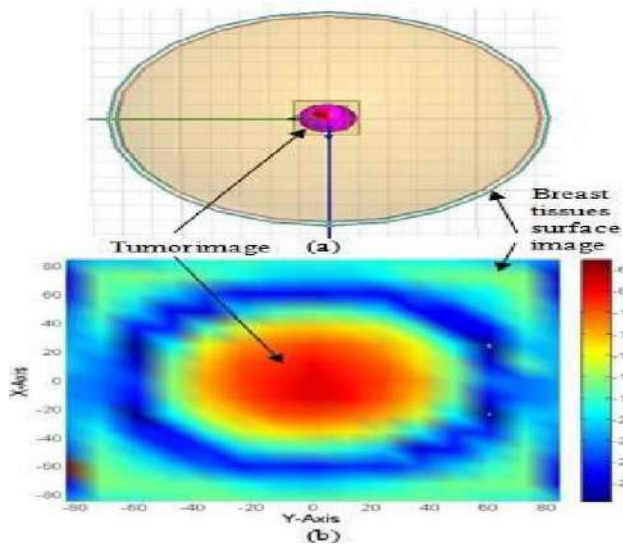


Figure 9: Position of the tumour inside the breast tissue structure (2D Image) (a) Top view of breast model (b) 2D Image for each breast tissue for different value of reflected power S11 value.

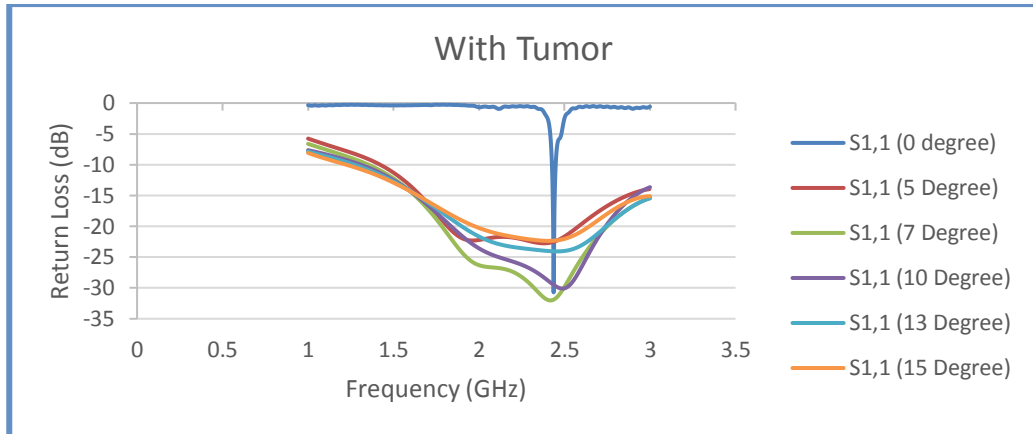


Figure 10: Comparison of S11 of the antenna array in all the bent degrees

Table 5: Outlines the overall antenna performance.

| Antenna Performances | | 0 Degree | 5 Degrees | 7 Degrees | 10 Degrees | 13 Degrees | 15 Degrees |
|----------------------|-----------------|----------|-----------|-----------|------------|------------|------------|
| Free Space | Frequency (GHz) | 2.408 | 2.404 | 2.382 | 2.386 | 2.396 | 2.514 |
| | S_{11} (dB) | -37.37 | -24.21 | -28.92 | -32.54 | -24.69 | -22.36 |
| On-silicon Bra | Frequency (GHz) | 2.436 | 2.380 | 2.418 | 2.488 | 2.456 | 2.406 |
| | S_{11} (dB) | -30.70 | -22.75 | -32.02 | -30.09 | -24.06 | -22.36 |

CONCLUSION

In this paper, we developed an array antenna designed to investigate the bending effect on breast tumour detection. The importance of the MWI has been emphasized and the configuration of the designed antenna was also presented. The result from the bending effect of the S-parameters shows that it has the capability for target detection.

ACKNOWLEDGEMENT

The authors would like to acknowledge Mr. Adegboye Olaolues Ayodeji of University of Uyo, Nigeria, for his technical help, and Rogers Corporation for their gift of Substrate material. The University of Uyo for their support for this work.

AUTHORS BIOGRAPHY

Ganadiko, M. Bayero is a student of Master of electronic engineering (Research), at Infrastructure University Kuala Lumpur (IUKL). He received his B.Sc degree in Electronics Engineering from IUKL. His research interest are Antenna Design. *Email: bayero12@yahoo.com*

Hon Kah Wye, PhD is a lecturer of Electronic engineering Department at IUKL. She has several years of teaching experience. His research interest are electronics & communication, Antenna Design and RF circuit Design.

Sanjay Sree is a lecturer of electronic engineering department at IUKL. He has several years of teaching experience. Her major field of study is Microwave, Microstrip Antenna, RF Circuit Design.

REFERENCES

- Islam *et al.*, 2017. Breast Phantoms for Estimation of Breast Tumor Using Microwave Imaging Systems. *IEEE Access* **6**, 78587–78597, <https://doi.org/10.1109/ACCESS.2018.2885087>.
- Ouerghi *et al.*, 2017, "Design and analysis of a microstrip antenna array for biomedical applications," *2017 International Conference on Advanced Technologies for Signal and Image Processing (ATSIP)*, Fez, 2017, pp. 1-5. doi: 10.1109/ATSIP.2017.8075589
- Khalil *et al.*, 2014. Inverse Scattering in Microwave Imaging for Detection of Malignant Tumor inside the Human Body. *International Journal of Signal Processing, Image Processing and Pattern Recognition*, 7(1), pp.135-144.
- Pierri *et al.*, 2000. *Second-order iterative approach to inverse scattering: numerical results*.
- Srinivasan *et al.*, 2019 Breast Cancer Detection Using Adaptable Textile Antenna Design. *Journal of Medical Systems*, 43(6).
- Shrestha *et al.*, 2012. Flexible Microstrip Antenna for Skin Contact Application. *International Journal of Antennas and Propagation*, 2012, pp.1-5.
- Zhong *et al.*, 2003. Microwave breast imaging: 3-D forward scattering simulation. *IEEE Transactions on Biomedical Engineering*, 50(10), pp.1180-118